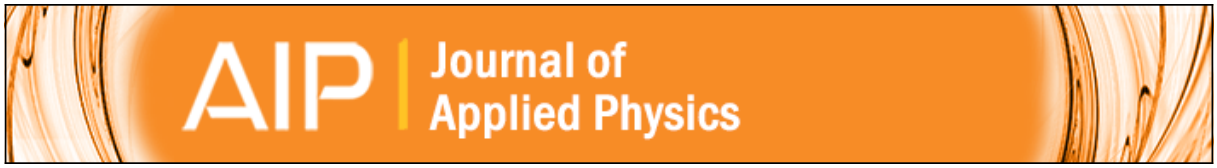

Thermal analysis, nuclear magnetic resonance spectroscopy, and impedance spectroscopy of N,N-dimethyl-pyrrolidinium iodide: An ionic solid exhibiting rotator phases

Josefina Adebahr, Aaron J. Seeber, Douglas R. MacFarlane, and Maria Forsyth

Citation: Journal of Applied Physics **97**, 093904 (2005); doi: 10.1063/1.1889245

View online: http://dx.doi.org/10.1063/1.1889245

View Table of Contents: http://scitation.aip.org/content/aip/journal/jap/97/9?ver=pdfcov

Published by the AIP Publishing

Thermal analysis, nuclear magnetic resonance spectroscopy, and impedance spectroscopy of N,N-dimethyl-pyrrolidinium iodide: An ionic solid exhibiting rotator phases

Josefina Adebahr[a] and Aaron J. Seeber
School of Physics and Materials Engineering, ARC Centre for Nanostructured Electromaterials, Monash University, Clayton 3800, Victoria, Australia

Douglas R. MacFarlane
School of Chemistry, ARC Centre for Nanostructured Electromaterials, Monash University, Clayton 3800, Victoria, Australia

Maria Forsyth
School of Physics and Materials Engineering, ARC Centre for Nanostructured Electromaterials, Monash University, Clayton 3800, Victoria, Australia

(Received 8 November 2004; accepted 17 February 2005; published online 20 April 2005)

N,N-dimethyl-pyrrolidinium iodide has been investigated using differential scanning calorimetry, nuclear magnetic resonance (NMR) spectroscopy, second moment calculations, and impedance spectroscopy. This pyrrolidinium salt exhibits two solid-solid phase transitions, one at 373 K having an entropy change, ΔS, of 38 J mol^{-1} K^{-1} and one at 478 K having ΔS of 5.7 J mol^{-1} K^{-1}. The second moment calculations relate the lower temperature transition to a homogenization of the sample in terms of the mobility of the cations, while the high temperature phase transition is within the temperature region of isotropic tumbling of the cations. At higher temperatures a further decrease in the ^{1}H NMR linewidth is observed which is suggested to be due to diffusion of the cations. © *2005 American Institute of Physics*. [DOI: 10.1063/1.1889245]

I. INTRODUCTION

Solid state conductors are of interest in the growing area of electrolytes for electrochemical devices such as batteries, fuel cells, sensors, and actuators. Ion conducting ceramics, polymer electrolytes, gels and glasses are materials that have been extensively investigated. Recently, the observation of fast-ion conduction in organic salts exhibiting rotator phases has led to an increased interest in these fascinating materials.[1]

The crystalline state of these materials is typically fully ordered at low temperatures, but as the temperature is increased they exhibit one or more solid–solid phase transitions, often due to the onset of different rotational motions. These transitions are usually associated with a large enthalpy and entropy increase. Some of these materials exhibit, in their highest temperature phase, plastic properties. In the plastic phase, the crystalline material flows readily under relatively low forces and can deform without fracture under stress.[2] In the early 1960s Timmermans proposed a criterion for the existence of plastic crystal phases, based on an investigation of organic molecular crystalline compounds such as cyclohexane, camphor, etc., which showed that the final entropy of melting, ΔS_f, is typically less than 20 J K^{-1} mol^{-1}.[3] Certain inorganic salts have also been found to exhibit rotator phases and sometimes also plastic behavior. Examples include Li_2SO_4 and Na_3PO_4, where "paddle-wheel" rotation of the anions while fixed on their lattice sites has been suggested as the cause of the long-range translational motion of the Li^+ and Na^+ cations.[4,5] Other organic-based materials with multiple phase transitions and rotator phases include families of quaternary-ammonium cations, imidazolium cations, and pyrrolidinium cations.[6–11]

The salts based on the N-alkyl-N-methyl-pyrrolidinium cations (Fig. 1) have been extensively explored in terms of phase behavior, conductivity, etc. The chemical structure of the salts, such as the choice of anion and/or the length of the alkyl chains, has been shown to greatly influence the properties of the materials. The iodide salts, for example, are usually solid at room temperature, exhibit fewer phase transitions, and have a higher melting point, compared to salts based on anions with a more delocalized charge such as PF_6^-, BF_4^-, or $N(SO_2CF_3)_2^-$. The melting point of the material de-

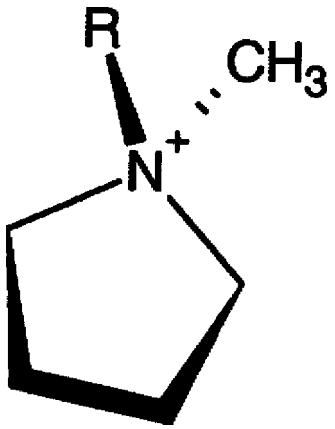

FIG. 1. Structure of the N-alkyl-N-methyl-pyrrolidinium cation.

[a]Author to whom correspondence should be addressed; electronic mail: josefina.adebahr@spme.monash.edu.au

creases as the length of the alkyl group increases, up to a certain length (which is dependent on the choice of anion).[1,11–17]

One method for determining the nature of molecular motion in these systems is nuclear magnetic resonance (NMR) second moment analysis. In order for this analysis to be accurately performed a crystal structure of the compound is desirable, where inter- and intra-molecular distances are known precisely. Crystal structure determination usually requires growth of a single crystal, which has been found to be a challenge in compounds with rotator or plastic crystal phases.[14] However, one example of a plastic crystal material from which it has been possible to grow a single crystal and where the crystal structure have been used for second moment calculations is tetramethylammonium dicyanamide, Me_4NDCA. In this case the heteronuclear dipolar interaction between the protons on the cation and the nitrogens and carbons on the dicyanamide anion was found to have a negligible contribution to the ^1H linewidth and the calculation was therefore based entirely on the homonuclear interaction (H–H) of the cations. The second moment for this highly symmetric cation was calculated for four different cases: a static cation, methyl group rotation on the cation, ratcheting (i.e., rotation of the cation around the C_2 or C_3 axis), and isotropic tumbling. The different rotational states of the cation were correlated to the experimentally determined ^1H NMR linewidth, showing that the cation exhibits rotational motions within the whole temperature range of investigation (182–390 K). At high temperatures the linewidth narrowed to values well below that for isotropic tumbling, which was attributed to the diffusion of the cation and correlated well with the conductivity.[18]

In our recent work, the pyrrolidinium family of salts have displayed both rotator phases and plastic crystal phases[11,13,14,19,20] although these have usually been observed for salts with delocalized charges on the anions, as mentioned above, as opposed to the more spherically symmetric iodide anion. The N,N-dimethyl pyrrolidinium cation is also of lower symmetry than the tetramethyl ammonium cation previously discussed. As such, isotropic tumbling may not be as easy to achieve. The second moment NMR analysis provides the ideal method to investigate the nature of the cation motions in the pyrrolidinium systems.

N,N-dimethyl-pyrrolidinium iodide is one of the simplest of the pyrrolidinium family members and a crystal structure has been determined,[14] and hence this system has been chosen as a model system in order to investigate the rotational and translational motions in these materials. These are then related to conductivity and phase behavior in the system.

II. EXPERIMENT

A. Samples

N,N-dimethyl-pyrrolidinium iodide, abbreviated $P_{11}I$, was prepared from 1-methyl pyrrolidine and iodomethane. For a detailed description of the synthesis method, see Ref. 11. The crystal structure of $P_{11}I$, used in the second moment calculations, was obtained by single crystal x-ray diffraction.

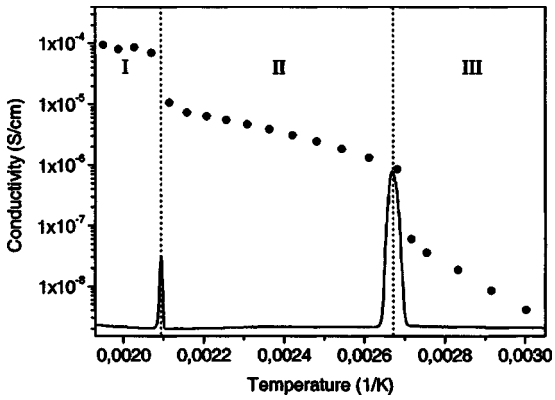

FIG. 2. Thermal behavior and conductivity as a function of temperature for $P_{11}I$.

The structures were solved by direct methods and refined by least squares, the hydrogen atoms were thereafter placed in calculated positions using a riding model. For a detailed description see Ref. 14.

B. Thermal analysis

A Perkin–Elmer differential scanning calorimeter (DSC) model 7 was used to measure the thermal properties of the sample, over a temperature range of 323–523 K with a scanning rate of 10 K min^{-1}.

C. Conductivity

Conductivity measurements were carried out on a Solartron frequency response analyzer model 1296, driven by SOLARTRON impedance measurements software version 3.2.0 over a frequency range of 1 MHz–0.01 Hz with a signal voltage of 0.1 V. The sample was pressed into a pellet and thereafter sandwiched between two stainless steel blocking electrodes. Measurements were taken every 10°, after a 3 min equilibration time. The cell temperature was controlled using a Eurotherm control model 2204. The temperature was measured using a type-*k* thermocouple with an accuracy of ±1 K. The conductance of the samples was determined from the real axis intercept in the Nyquist plot of the impedance data.

D. NMR spectroscopy

^1H NMR linewidth measurements were performed on a Bruker AS300 pulse NMR spectrometer operating at a Larmor frequency of 300.14 MHz, using a single $\pi/4$ pulse of 1.5 μs, a recycle delay of 6 s, and 32 scans. At all temperatures, the probehead was allowed to equilibrate for 20 min before tuning and data collection.

The peaks were fitted to Gaussian line shapes. The error is estimated to be less than 10%.

III. RESULTS AND DISCUSSION

The DSC trace and the conductivity of the sample are plotted as a function of temperature in Fig. 2. The thermal analysis shows two exothermic solid–solid transitions; one at 373 K ($\Delta S = 38$ J K^{-1} mol^{-1}) and one at 478 K (ΔS

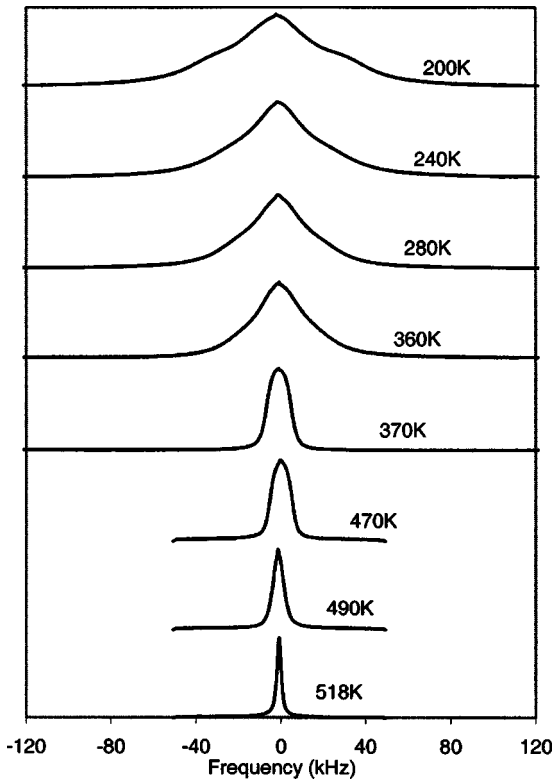

FIG. 3. Representative single-pulse static ^{1}H NMR spectra for $P_{11}I$ as a function of temperature.

$=5.7\ \mathrm{J\,K^{-1}\,mol^{-1}}$). No transitions were observed at lower temperatures, and the sample decomposed before melting at temperatures above the second phase transition. The high temperature phase is denoted phase I, the middle phase, II, and the low temperature phase, III. The size of ΔS for the III$\rightarrow$II transition suggests a sudden onset of additional degrees of freedom leading to greater entropy in phase II, while the II$\rightarrow$I transition gives a more modest change in entropy. (Typically, the total entropy of fusion from the low temperature ordered phase of related pyrrolidinium salts is $40-50\ \mathrm{J\,K^{-1}\,mol^{-1}}$ hence the measurements suggest that phase I is already close to the liquid state in entropic terms.) Interestingly, this will be shown to be consistent with the significance of the changes in NMR linewidth discussed below. It is clearly seen that there is a step increase in conductivity at the same temperature that the phase transitions occurs.

Figure 3 shows selected 1-pulse static ^{1}H NMR spectra for the $P_{11}I$ sample. It is immediately apparent from inspection of these spectra that at lower temperatures, two dynamic states for the P_{11}^+ cation are found. The spectra have been deconvoluted in order to extract the linewidth and relative area from each component. The spectra were fitted using Gaussian functions.

The full width half maximum (FWHM) and percentage of total spectral area for the two peaks in the ^{1}H spectra are presented as a function of temperature in Figs. 4 and 5, respectively, allowing the changes in the relative areas and linewidths of the two peaks to be seen in more detail. From Fig. 5 it is evident that the relative area of the broad component of the ^{1}H NMR spectra drops slowly from a maximum

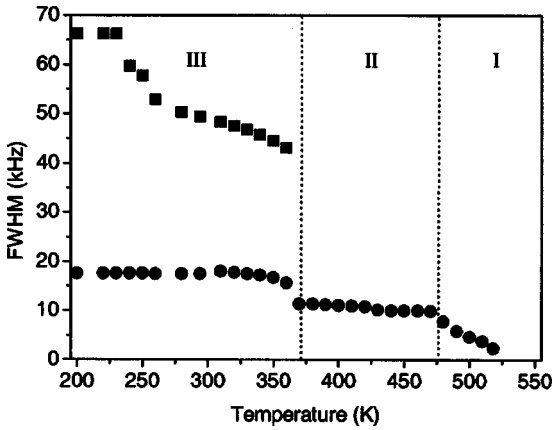

FIG. 4. FWHM as measured for the broad (■), and narrow (●) peaks found in the static ^{1}H NMR spectra at different temperatures for $P_{11}I$.

$>$90% at 210 K to $\sim$80% above 300 K, and then remains relatively constant until disappearing suddenly around 370 K. At this temperature, a small decrease in the linewidth of the narrow component is also observed, from 16 to 11 kHz. Above 470 K, the linewidth of this component drops steadily, and reaches 2.4 kHz at 518 K, the maximum temperature reached.

M_2 calculations

Second moment calculation on the basis of a crystal structure is a standard procedure and has been used widely to determine theoretical linewidths for different rotational motions. From the crystal structure of the $P_{11}I$ material, a second moment analysis of the linewidths is possible, using the Van Vleck's equation, assuming that the magnetic dipolar interaction is the only interaction between the spins:

$$M_2 = \left(\frac{\mu_0}{4\pi}\right)^2 \hbar^2 \frac{1}{N}\left[\frac{3}{5}\sum_{j,k}\gamma_k^4 I_k(I_k+1)r_{jk}^{-6} + \frac{4}{15}\sum_{j,f}\gamma_k^2\gamma_f^2 I_f(I_f+1)r_{jf}^{-6}\right], \quad (1)$$

where N is the number of resonant nuclei over which the second moment is calculated, γ is the gyromagnetic ratio, j and k are the resonant species, and f are the nonresonant species, I is the spin, and r is the internuclear distance. This

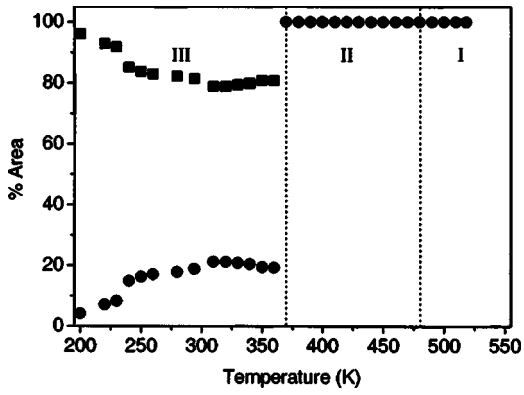

FIG. 5. Relative percentage of the area of the broad (■) and narrow (●) peaks found in the static ^{1}H NMR spectra at different temperatures for $P_{11}I$.

TABLE I. The FWHM at different temperatures for the broad and narrow components in the ^{1}H spectra of $P_{11}I$.

Temperature (K)	LW broad (kHz)	LW narrow (kHz)
200	66	22
230	66	18
240	60	18
280	50	18
360	43	16
370	···	11
470	···	10
490	···	6
518	···	2

equation gives the theoretical static second moment. To take into account the effect of reorientation of the methyl groups on the second moment, the intramethyl internuclear sums in Eq. (1) are modified by the factor

$$\tfrac{1}{4}(3\cos^2\phi - 1)^2, \tag{2}$$

where ϕ is the angle between the internuclear vector and the axis of rotation. Finally, in the case of fully isotropic tumbling all protons are averaged to the center of mass of the molecule and only intermolecular components of the interaction remain.

Using the following relation, the theoretical linewidth can then be calculated:

$$\Delta\nu_{\mathrm{FWHM}} = \frac{\sqrt{2\ln M_2}}{\pi}. \tag{3}$$

The calculations were based on the crystal structure of $P_{11}I$, using a cutoff distance of 1 unit cell in each direction (i.e., the calculation involves all interactions between all atoms within one central unit cell, and with 26 surrounding unit cells). This method has previously been used for calculation of the second moment on a similar system.[18] Due to the small gyromagnetic ratio of ^{127}I and ^{14}N, and the low abundance of ^{13}C, contributions from the nonresonant nuclei were assumed to be small, and were not included in the calculations. The second moment, and theoretical linewidths, have been calculated for $P_{11}I$ where the P_{11}^+ cations are static, where the methyl groups on these cations are spinning, and where the cations are tumbling isotropically, giving a FWHM of the static ^{1}H NMR spectra of 66, 54, and 5.4 kHz, respectively. Such linewidths were calculated assuming that increases in the lattice parameters of this material are negligible. Table I contains the experimental linewidths for the broad and the narrow components at different temperatures. Comparing the experimentally found linewidths with those calculated from the second moment, it can be seen that below 230 K the broad component of the ^{1}H spectra represents static P_{11}^+ cations, and that above this temperature the methyl groups on these cations begin to rotate. The transition from static cations to where the methyl groups are spinning is gradual, and it is not expected that such a transition would be visible in DSC. Between 370 and 470 K the FWHM linewidth remains approximately at 11 kHz which is too high for the P_{11}^+ cation to be undergoing isotropic tumbling, but clearly a significant degree of rotation must be occurring in order to account for the narrowing of the linewidth, compared to purely methyl group rotations. One obvious type of rotation may occur around the "C_2 axis" that bisects the ring and passes through the nitrogen (the pyrrolidinium ring is not completely flat and therefore formally no C_2 axis exists). The second moment calculation for this type of rotation gave a theoretical linewidth of 22 kHz, which is still higher than the experimental linewidth of 11 kHz. It is likely that in this temperature region a number of different motions may be experienced by the cation species, as was the case in the Me_4NDCA where both isotropic tumbling and ratcheting motions were postulated to occur simultaneously.[18] A mixture of isotropic tumbling and rotation around the C_2 axis of the cations could be the explanation for the observed linewidth of 11 kHz as could a hindered form of isotropic rotation in which some reorientations are more probable than others. A change in the lattice dimensions compared to the low temperature structure could also account for part of the lower than expected value for the rotation around the C_2 axis. Above 470 K, the steady decrease in the linewidth is indicative of a transition to isotropic tumbling of the P_{11}^+ cations, with the decrease in linewidth below 5.4 kHz probably being due to translational motion of the cation.

The DSC transition found at ~373 K in this sample is followed by a change in dynamic state of the P_{11}^+ cations. The broad component in the NMR spectrum disappears suddenly at this temperature, indicating a homogenization of the system, where all cations now have an increased and equivalent mobility. Above this transition (in phase II), the linewidth indicates motions which appear to be at least in part isotropic tumbling. An accelerated rate of vacancy formation in phase II as a result of its higher energy thermodynamic state would account for the decrease in activation energy observed for the conduction process. The II→I transition at ~478 K does not correspond to any sudden transitions in the NMR spectra, however the rate of change of linewidth as a function of temperature is slow, perhaps indicating the progressive onset of rapid diffusional motions in phase I. The NMR linewidths at temperatures around 490 K and above are in accordance with the second moment calculations for isotropic tumbling of the P_{11}^+ cations, indicating that the onset of isotropic motions is completed. Whether or not this phase also exhibits plastic mechanical properties has yet to be determined. Given that the melting transition is not observed due to decomposition prior to melting, Timmermans' criterion cannot be applied in this case. However, the sample is not observed to deform at all when taken up to temperatures above the II→I phase transition in the conductivity cell.

A previous system which has shown high ion mobility but not necessarily plastic behavior is ethyl–methyl–imidazolium iodide (EtMeImI). This material has displayed some of the highest solid state conductivity values measured to date in organic materials, and this was linked to the diffusion of the imidazolium cation.[21] A similarity between $P_{11}I$ and EtMeImI is the tunneled crystal structure. The anions can be regarded as more or less immobile, creating a static matrix in which the cations are free to move in the rotator

phases. If the packing is loose then molecular rotations could be relatively easy and the presence of vacancies would allow hopping of the cations between sites.[21]

If we regard the iodide anions to be immobile in the lattice, then it follows that, though vacancies may facilitate the movement of single cations, in order for a plastic deformation to occur, the anions need to be able to move as well. It has been shown that, in many plastic crystals, the anions and cations are equally mobile.[22] A static anion matrix, within which the cations are free to move, has been found for other systems such as AgI and AgI–CuI mixtures where the Ag ions moves in a static iodide environment, creating high cation transport number and high conductivity.[23,24] Thus these organic iodides represent an interesting class of compounds which exhibit rotator phase because of rotational motions of one of the ions while apparently not being plastic, possibly as a result of the rigidity of the lattice associated with the other ion.

IV. CONCLUSIONS

The combination of second moment calculation and NMR linewidth measurements has been used in order to investigate changes in ionic mobility followed by the phase transitions in this model system. There is an increased mobility from the static phase at low temperatures to the spinning of the methyl groups starting at ~230 K. The first phase transition observed in the DSC, occurring at 373 K, is associated with a change in the dynamic state of the P_{11}^{+} cations. In phase II the motions of the cations appear to be at least in part isotropic tumbling, and an accelerated rate of vacancy formation in this phase is likely to be the reason for the observed decrease in activation energy for the conductivity. At temperatures above 490 K the linewidth decreases below the value calculated for isotropic tumbling. This is attributed to the onset of translational motion (diffusion) of the cations. Furthermore, it is suggested that this member of the pyrrolidinium family does not exhibit plastic properties in the temperature range investigated, in contrast to other salts based on the same cation, e.g., $P_{11}BF_4$ and $P_{11}PF_6$, where the anion also appears mobile.

ACKNOWLEDGMENTS

This work was funded by the Australian Research Council under the ARC Centres of Excellence program and through ARC Discovery projects.

[1] D. R. MacFarlane, J. H. Huang, and M. Forsyth, Nature (London) **402**, 792 (1999).
[2] J. N. Sherwood, "The crystal structure of some plastic and related crystals," in *The Plastically Crystalline State*, edited by J. N. Sherwood (Wiley, New York, 1979).
[3] J. Timmermans, J. Phys. Chem. Solids **18**, 1 (1961).
[4] R. Aronsson, B. Jansson, H. E. G. Knape, A. Lunden, L. Nilsson, C. A. Sjoblom, and L. M. Torell, J. Phys. (Paris), Colloq. **41**, C6/35 (1980).
[5] D. Wilmer, K. Funke, M. Witschas, R. D. Banhatti, M. Jansen, G. Korus, J. Fitter, and R. E. Lechner, Physica B **266**, 60 (1999).
[6] M. Hattori, S. Fukada, D. Nakamura, and R. Ikeda, J. Chem. Soc., Faraday Trans. **86**, 3777 (1990).
[7] T. Tanabe, D. Nakamura, and R. Ikeda, J. Chem. Soc., Faraday Trans. **87**, 987 (1991).
[8] S. Iwai, M. Hattori, D. Nakamura, and R. Ikeda, J. Chem. Soc., Faraday Trans. **89**, 827 (1993).
[9] H. Ishida, Y. Furukawa, S. Kashino, S. Sato, and R. Ikeda, Ber. Bunsenges. Phys. Chem. **100**, 433 (1996).
[10] T. Shimizu, S. Tanaka, N. Onoda Yamamuro, S. Ishimaru, and R. Ikeda, J. Chem. Soc., Faraday Trans. **93**, 321 (1997).
[11] D. R. MacFarlane, P. Meakin, J. Sun, N. Amini, and M. Forsyth, J. Phys. Chem. B **103**, 4164 (1999).
[12] M. Forsyth, J. Huang, and D. R. MacFarlane, J. Mater. Chem. **10**, 2259 (2000).
[13] S. Forsyth, J. Golding, D. R. MacFarlane, and M. Forsyth, Electrochim. Acta **46**, 1753 (2001).
[14] J. Golding, N. Hamid, D. R. MacFarlane, M. Forsyth, C. Forsyth, C. Collins, and J. Huang, Chem. Mater. **13**, 558 (2001).
[15] J. H. Huang, M. Forsyth, and D. R. MacFarlane, Solid State Ionics **136**, 447 (2000).
[16] D. R. MacFarlane and M. Forsyth, Adv. Mater. (Weinheim, Ger.) **13**, 957 (2001).
[17] J. Sun, D. R. MacFarlane, and M. Forsyth, J. Mater. Chem. **11**, 2940 (2001).
[18] A. Seeber, M. Forsyth, C. Forsyth, S. Forsyth, G. Annat, and D. R. MacFarlane, Phys. Chem. Chem. Phys. **5**, 2692 (2003).
[19] J. Efthimiadis, S. J. Pas, M. Forsyth, and D. R. MacFarlane, Solid State Ionics **154**, 279 (2002).
[20] J. Efthimiadis, G. J. Annat, M. Forsyth, and D. R. MacFarlane, Phys. Chem. Chem. Phys. **5**, 5558 (2003).
[21] H. A. Every, A. G. Bishop, D. R. MacFarlane, G. Orädd, and M. Forsyth, J. Mater. Chem. **11**, 3031 (2001).
[22] M. Forsyth, J. Pringle, D. R. MacFarlane, and W. Ogihara, "Ion conduction in organic plastic crystals; in *Ionic Liquid: The Front and Future of Material Development, (Ionsei Ekitai)*, edited by H. Ohno (CMC Publishing Co., Ltd, Tokyo, 2003), pp. 144.
[23] A. K. Ivanov-Schitz, B. J. Mazniker, and E. S. Povolotskaya, Solid State Ionics **159**, 63 (2003).
[24] J.-S. Lee, S. Adams, and J. Maier, J. Phys. Chem. Solids **61**, 1607 (2000).